ICE SURFACE AND BEDROCK TOPOGRAPHY IN COATS LAND AND PART OF DRONNING MAUD LAND, ANTARCTICA, FROM SATELLITE IMAGERY

P. D. MARSH

British Antarctic Survey, Natural Environment Research Council, High Cross, Madingley Road, Cambridge CB3 0ET, UK

ABSTRACT. Near-infrared images from Landsat MSS Band 7 and NOAA Very High Resolution Radiometer channel 2 give a synoptic view of ice surface features in Coats Land and western Dronning Maud Land. Comparison with survey data collected by ground parties shows that the most prominent features, with wavelengths between 2 and 10 km, are undulations with slope changes as small as 0.5°. The imagery permits the mapping of zones with similar surface topography, which outline shapes of the glaciers feeding Filchner Ice Shelf, and topographic highs associated with exposed mountain ranges. The relationship of the undulations to these major features, and published radio-echo sounding data, support the conclusion of workers elsewhere that the surface undulations are mainly related to bottom topography. Discontinuities in the surface topography are inferred to indicate discontinuities in bedrock morphology and are used to suggest the location of subglacial scarps and other changes in bedrock elevation. The orientation of the inferred bedrock features suggests that many are fractures associated with Mesozoic rifting along the Weddell Sea and Filchner Ice Shelf margins of the continent.

INTRODUCTION

The major glaciers that drain a large part of the Dronning Maud Land sector of Antarctica (Fig. 1) and feed Filchner Ice Shelf (Levanon and Bentley, 1979; Crabtree and Doake, 1980) flow westward through Coats Land. Between them the ice sheet rises in ridges up to 1000 m higher than the glacier surfaces (Fig. 2). Almost all of the groups of mountains and nunataks in the region have been topographically and geologically surveyed. Although associated subglacial bedrock highs are shown in broad outline on maps of the bedrock surface (e.g. Grikurov, 1978; Drewry and Jordan, 1983), both topographic and non-interpretative geological maps are mainly blank outside outcrop areas. In this paper the survey data and descriptions given by ground parties, and US Navy tricamera air photography, are used to identify the nature of features seen in satellite images.

The images used were paper prints from either Landsat Multispectral Scanner (MSS) Band 7 (0.8–1.1 μm, nominal resolution 80 m) or US National Oceanic and Atmospheric Administration weather satellite Very High Resolution Radiometer (VHRR) channel 2 (0.725–1.1 μm, nominal resolution 1.1 km). They give a synoptic view of small scale ($<$ 10 km wavelength) surface undulations, which is used to describe the major geographical features beyond areas where they are known from the ground-based surveys. The undulations are of the same scale as those that have been shown to be related to bottom topography (Budd and Carter, 1971; Thorarinsson and others, 1973). Their distribution in the area described here is used to make inferences as to the form of the subglacial bedrock landforms associated with the major glaciers and the exposed mountain ranges.

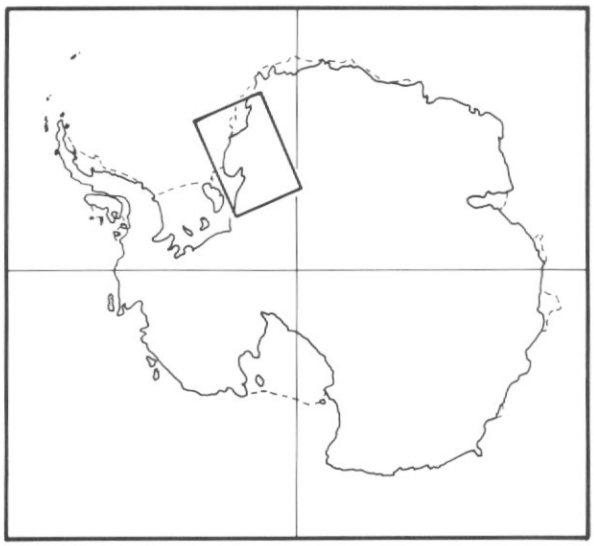

Fig. 1. The location within Antarctica of the area studied.

Representation of surface features in the satellite images

Satellite images of the Antarctic ice sheet provide a clear representation of small-scale surface features (Swithinbank, 1977). This is due to a fortunate combination of three main factors: low sun angles, which make the amount of surface illumination very sensitive to changes in slope, the flow of ice, which tends to inhibit the formation of surface forms sufficiently steep to cast shadows, and the relatively uniform reflectance of snow, which minimizes the effect in the images of non-topographic surface changes.

In the Landsat images used, the sun elevation (θ) varies between 8° and 27°. For the low surface slopes involved ($< 5°$) and $\theta = 8°$, a 1° change in the angle of incidence produces a 12% change in the amount of radiation reaching a surface. At $\theta = 27°$, only a 3.5% change is produced. However, where overlapping coverage contains seasonal variations in θ there appears to be no major change in the ease with which the same features are recognized, or in the number of features seen. The effect of surface slope on the angle of incidence is dependant on sun azimith (ϕ). Slope changes measured parallel to ϕ produce the changes in illumination quoted above, whereas those at right angles to ϕ have negligible effect. Hence linear features with trends sub-parallel to ϕ are effectively invisible. However, the range of ϕ available in VHRR images provides reassurance that no bias in the recognition of major features results from the unchanging ϕ of Landsat (85° in the centre of the area studied). For reasons given below little attention will be given to the orientation of most small scale features, hence any bias in the apparent distribution of their trends is of minor importance.

The most prominent features in the Landsat imagery have wavelengths between 2 and 10 km. Barometric altitude profiles across parts of Coats Land (Bailey and Evans, 1968, fig. 6; Peel, 1976, fig. 1 b) show that these gradations in image density correspond to features with slope changes as small as 0.5° (e.g. height 7 m at wavelength 5 km). At scales nearer the resolution of the imagery only steeper features are apparent – a series of undulations of wavelength 0.5 km on Brunt Ice Shelf, surveyed by Coslett and others (1975), become indistinct when the slope change across them is about 1° (height about 1.5 m). The smallest features seen are crevasses, some of which may be

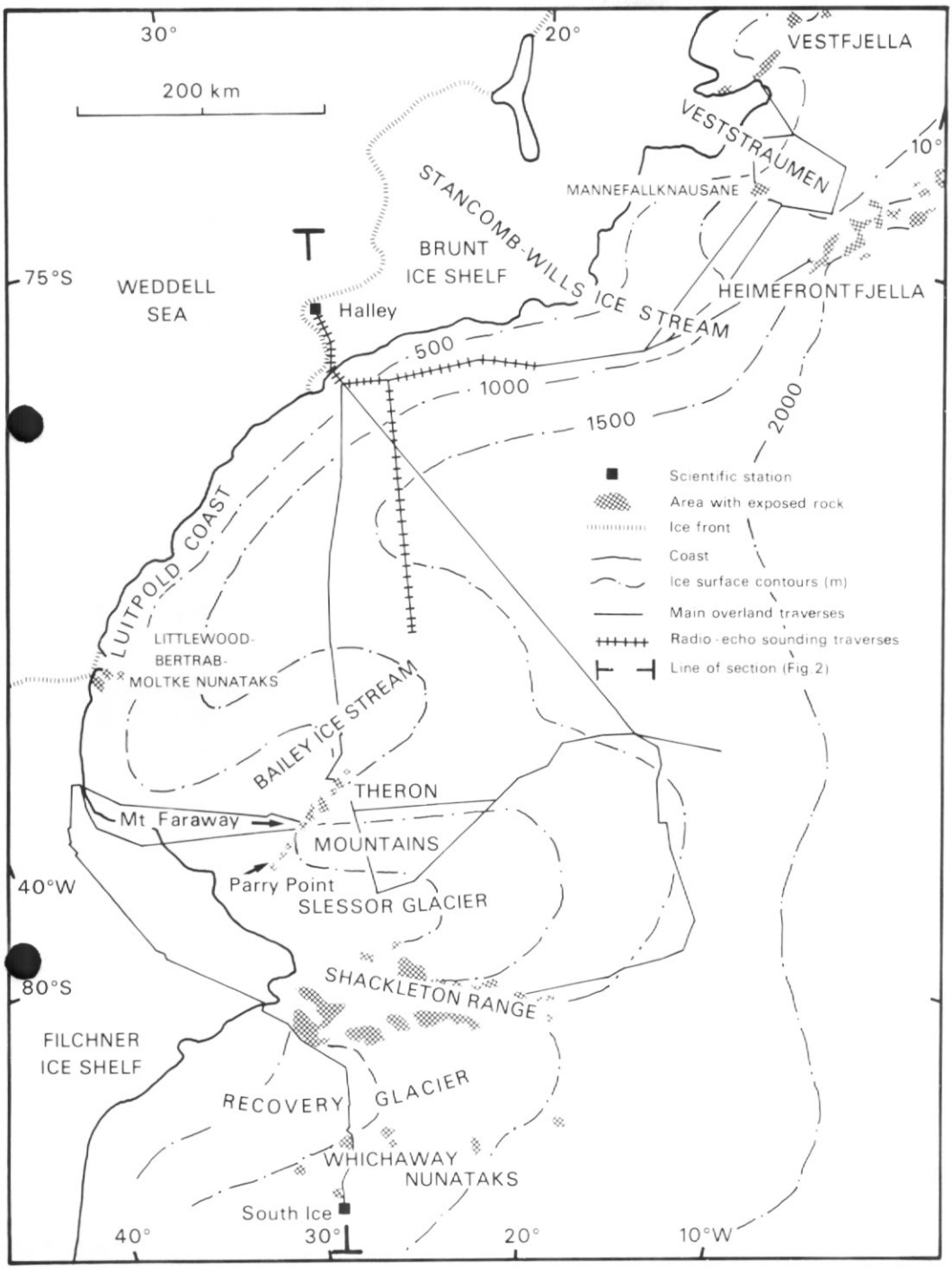

Fig. 2. Coats Land (west of 20° W) and part of Dronning Maud Land (east of 20° W) showing place names mentioned in the text, ice surface contours and the routes of major overland traverses.

narrower than the nominal resolution of the imagery (Crabtree and Doake, 1980). They give very dark image tones, probably due to areas of shadow. In VHRR images, features with wavelengths as short as 3 km, associated with slope changes of 1–2°, are visible in many cases. Larger features, for example a series of undulations across the upper Slessor Glacier with wavelength 8 km and height *c.* 23 m (from Peel, 1976, fig. 1 b), are seen in almost all images.

In Landsat images features more than about 30 km across are often difficult to distinguish due to the disordering of already small changes of image tone by superimposed smaller scale features. An upper limit to the scale of landforms that can be recognized reliably is imposed by the change in θ with the curvature of the earth, which is of the same order as slope changes about landforms more than about 100 km across. The lower resolution of VHRR images makes changes in illumination across large scale features more apparent, and those due to regional landforms are detectable in some images. However, although the large area covered (*c.* 1800 km cross track) allows them to be viewed in the context of the earth's curvature, it is difficult to get a reliable estimate of shape.

The review of the optical properties of snow given by Warren (1982) indicates that for the near-infrared wavelengths of interest, variations in reflectance of about 30% may occur due to changing grain size. Variations of this magnitude are mainly seasonal but changes of the same order as changes in illumination can be expected, for example due to variations in the distribution of new snow. Such variations are probably indicated by irregular areas (representing several thousand square kilometres) of slightly darker image tone in two images taken on successive days of an area north of the Theron Mountains. Some, but not all, of the (non-gradational) margins change between the images; the change in image tone is similar in magnitude to the smaller topographic changes. Other images provide less convincing examples but all appear to be superimposed on changes due to topography; they resemble a chemical stain on a photographic print. A change in reflectance *coincident* with a topographic feature was suggested by Martin and Sanderson (1980) to account for rapid changes in image density at ridges on ice rises. Martin and Sanderson (1980, p. 44) point out that the 'distinct apparent shadow' is inconsistent with the sun angle and the measured change in surface slope. However, in near-infrared imagery true shadows are effectively opaque, and the author has the impression not of shadow but of a rapid change in illumination due to a local increase in curvature, which *is* present on the summit of the ice rise discussed by Martin and Sanderson.

The most dramatic differences in reflectance are observed where bare ice is exposed by ablation or where melt water is present (Swithinbank and Lane, 1977). Such areas give image tones darker than all others except for shadow and those free of snow or ice. In MSS band 7 images of Coats Land they are bounded by changes in tone more abrupt than those associated with slope changes around topographic features of similar size. The only other features known not to be directly related to slope changes are dark areas in zones of extensive crevassing. These are assumed to be due to unresolved areas of bare ice and/or shadow.

In summary it can be stated that almost all of the features on the ice surface seen in the images are due to surface undulations, and that almost all of those that are not can be recognized as such. Comparison with air photographs, local survey data and descriptions given by observers on the ground suggests that the overall form of features between 2 and 15 kilometres across is more easily estimated from the remote viewpoint and 'hill shading' provided by Landsat than from observations made from the ground or from aircraft. The most significant limitation in image interpretation arises from difficulty in recognizing regional slopes; for example, a series of terraces on a slope cannot be reliably distinguished from ridges on a horizontal surface.

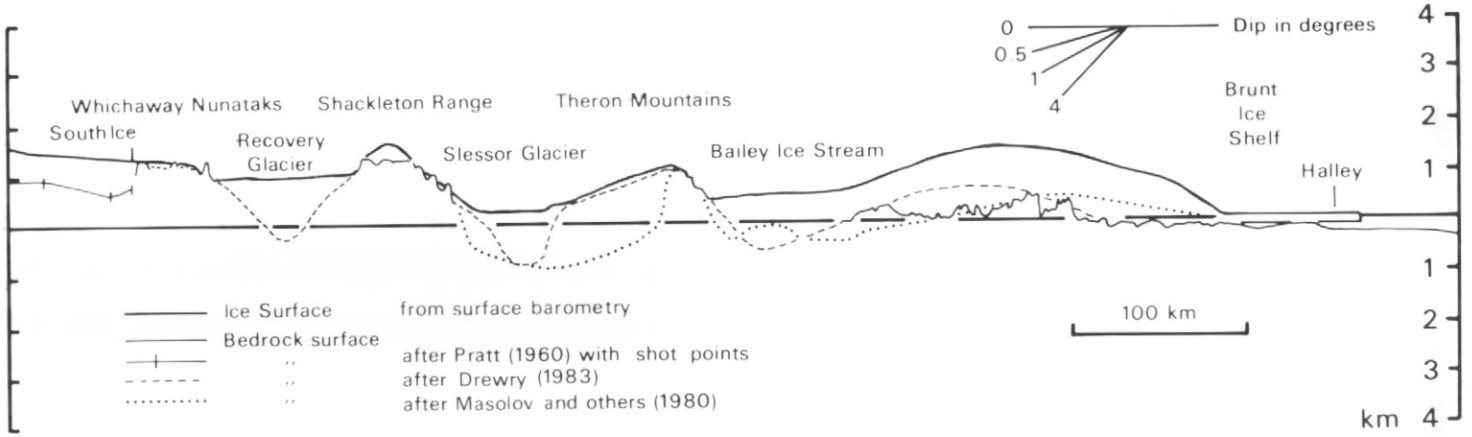

Fig. 3. Ice surface and bedrock profiles along a line passing through South Ice and Halley. See Fig. 2 for line of section.

In the following descriptions 'wavelength' refers to the smallest dimension and for non-periodic forms is the distance over which the image tone varies from that of the surroundings. The wavelength or wavelength range given refers to typical features; most areas have a limited range of wavelengths. The 'longitudinal features' on glaciers are similar to the 'flow lines' described by Crabtree and Doake (1980), and are taken to be parallel to the flow. In referring to the altitude profiles 'amplitude' is the variation about the regional slope rather than height differences on individual features.

Surface Topography

The general form of the ice surface is shown in Fig. 2; the contours are modified from Drewry (1983) with the addition of barometric altitude data collected during overland traverses from Halley (Samuel, 1968*a*, *b*; Noble, 1968; N. W. Riley m.s. map; routes shown in Fig. 2) and BAS survey data from the main mountain ranges (given in precis by Worsfold, 1967, fig. 1; Juckes, 1968, fig. 2; Brook, 1972a, fig. 1; and Skidmore and Clarkson, 1972, fig. 1). The traverse data provide an almost complete surface profile close to 29° W (Fig. 3). Zones with similar surface topography revealed by the imagery are outlined in Fig. 4, in which their positions are fixed using a graticule based on the Doppler satellite positions of Sturgeon and Renner (1983). The morphology of the ice surface, and the bedrock surface where known, are described from south to north, using a combination of 'ground truth' from overland and air surveys, and satellite image interpretation. The most striking variations in ice surface topography occur in the region of the Theron Mountains and Shackleton Range. The image mosaic of this area (Fig. 5) illustrates almost all of the types of feature and terrain recognized elsewhere and the convention adopted for their representation in Fig. 4.

Whichaway Nunataks (*areas* 1 *A and* 1 *B in Fig.* 4)

The main group of nunataks was surveyed by the Commonwealth Trans-Antarctic Expedition 1955–58 (TAE) (Blaiklock and others, 1966) but the remainder of the area, which is outside the orbital range of Landsat (80° N–80°S), has been mapped only from distant oblique air photographs. Fig. 6 was drawn from tricamera photography using control points in the Shackleton Range and a few observations made towards the nunataks during a survey of the range (A. True and C. A. Clayton, unpublished survey notes). These data position the nunataks *c.* 2 km to the north of the position given by Blaiklock and others (1966).

Areas 1A and 1B have localized rock outcrop and irregularly distributed ice features of wavelength 1 km. They are separated by a tributary of Recovery Glacier, which is marked by crevasse zones and by an absence of short wavelength features. It appears to be only a little lower than the adjacent areas. At Recovery Glacier the ice features in areas 1A and 1B cease abruptly and the central part of the northern boundary of area 1A is a 'precipitous tumbling slope of ice (Fuchs and Hillary, 1958, p. 104) about 75 m high. No clear boundary with the polar plateau rising to the south is seen but an indistinct north-west trending feature (Fig. 4) visible in VHRR imagery meets Recovery Glacier at about 32° W, where there appears to be an increase in the influx of ice from the south.

Nunataks in area 1A are horizontally bedded sedimentary rocks (Stephenson, 1966). The largest group are conical hills, the highest of which (Hopalong Nunatak *c.* 1375 m) overlooks Recovery Glacier and has rock outcrops extending down to only a few metres above the glacier surface at *c.* 980 m. Most of the other nunataks near

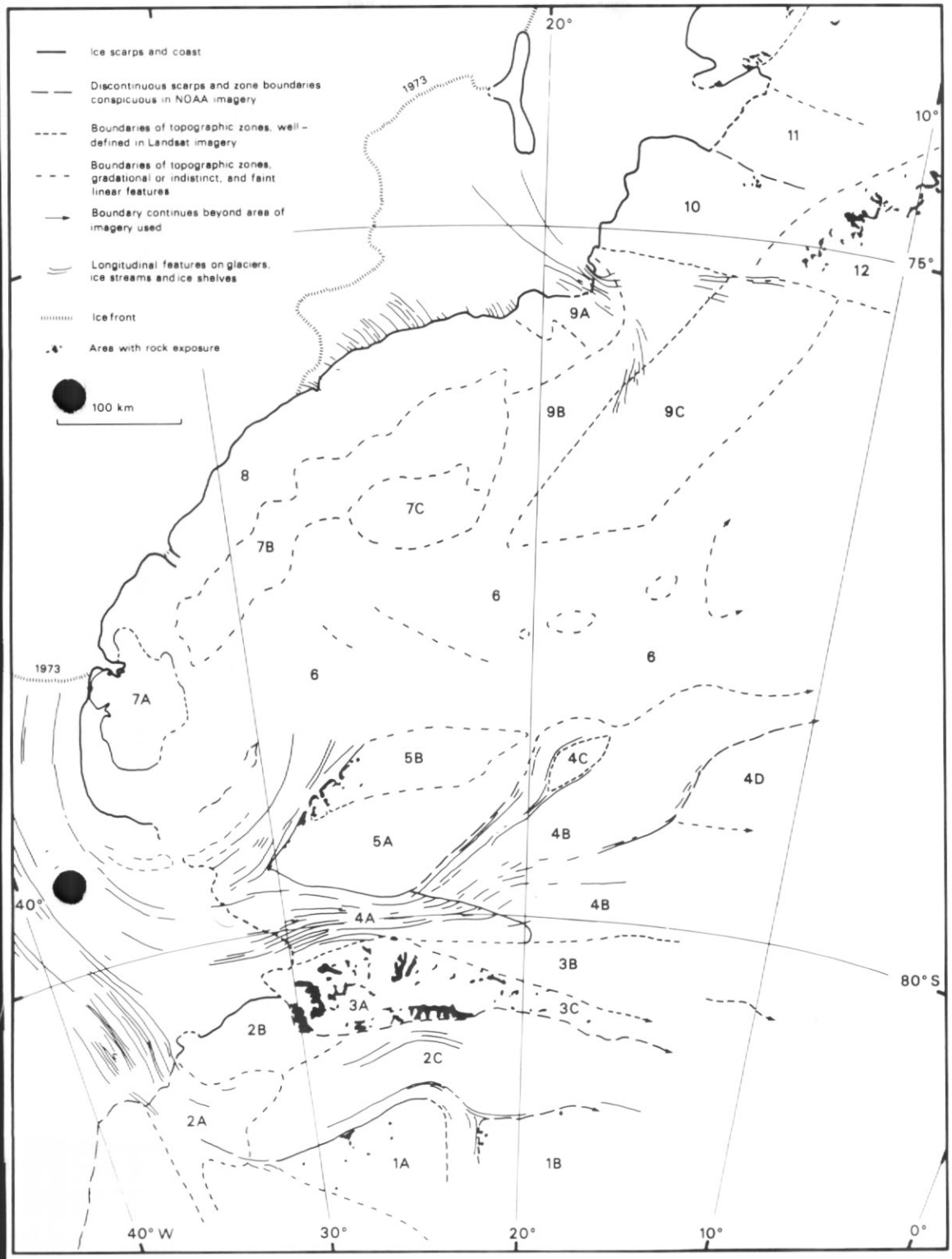

Fig. 4. Ice surface features and boundaries of physiographic zones recognized from the imagery.

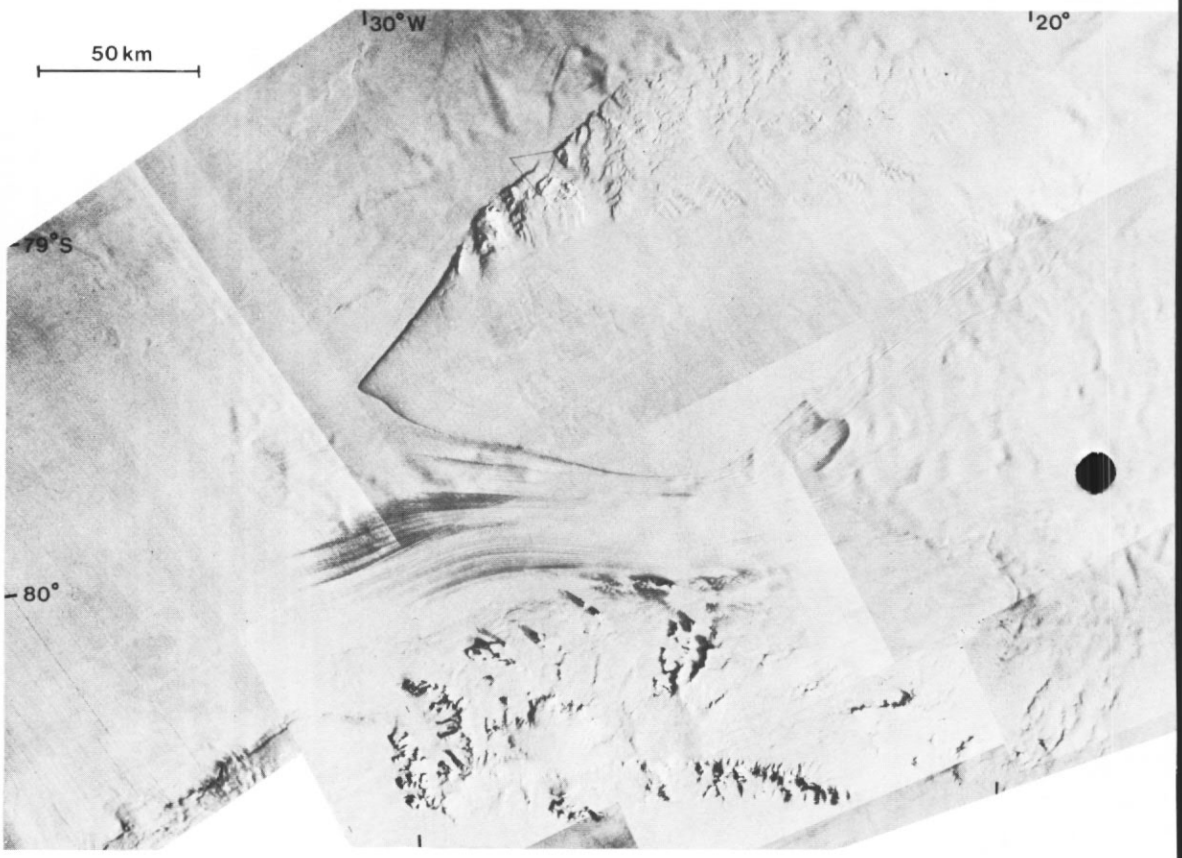

Fig. 5. Landsat mosaic of the Shackleton Range–Theron Mountains area. The triangle in the Theron Mountains marks USGS Doppler satellite station 22207 (Sturgeon and Renner, 1983).

the TAE traverse have summits between 1100 and 1300 m but many of these rise only a few metres above the ice. Seismic soundings from South Ice (Fig. 2) (Pratt, 1960) indicate that the bedrock there descends to below 1000 m above sea level (Fig. 3).

Nunataks in area 1B lack the conical form of those in area 1A, and the eastern most exposures appear to be the rim of a flat-topped sub-ice escarpment. The western group are only a few metres above the ice, which balloon altimetry (Levanon and Bentley, 1979) indicates to be at around 1500 m.

Recovery Glacier (areas 2A, 2B, and 2C)

The southern boundary of this glacier is marked by zones of intense crevassing. The scarp at the boundary decreases in height towards the east but the crevasse zones show the glacier to extend for many tens of kilometres to the east along an ice surface valley mapped by Levanon and Bentley (1979). In contrast, the northern margin is indistinct and when crossing from the north the TAE (Fig. 2) did not encounter heavy crevassing until the first longitudinal features shown in Fig. 4 were reached. These are ridges and furrows associated with zones of crevassing and pressure hummocks up to 24 m high (Fuchs and Hillary, 1958; Blaiklock and others, 1966, Sheet W81 28/30). Their trends

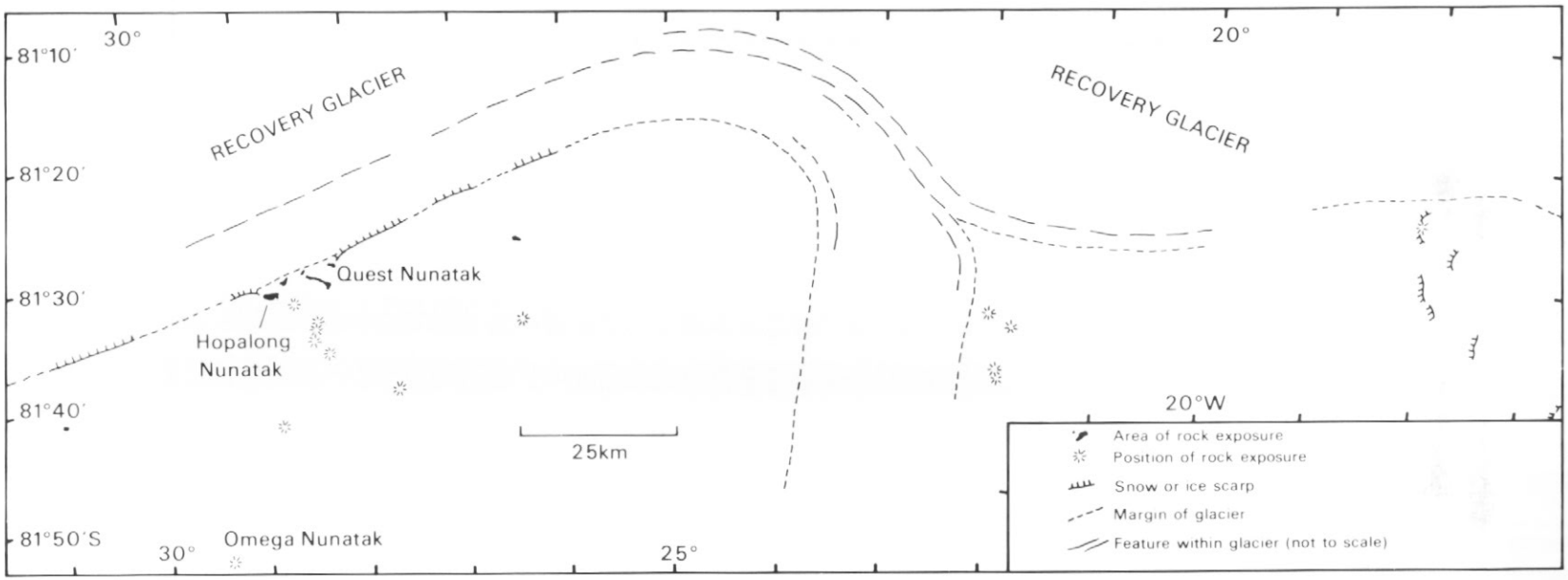

Fig. 6. Sketch map of the Whichaway Nunataks and the southern margin of Recovery Glacier.

suggest that between about 16° W and 34° W the main flow of the glacier remains roughly parallel to the southern boundary. It appears to sweep westwards through area 2 A whilst area 2 B receives ice derived mainly locally from the Shackleton Range. This interpretation is supported by the pattern of flow lines on the Filchner Ice Shelf (Fig. 4; and see Crabtree and Doake, 1980). A large proportion of the ice joining the glacier from the south appears to flow around, rather than over, areas 1 A and 1 B.

In VHRR imagery area 2 A is seen to be dominated by mainly northward trending features of wavelength around 8 km and broad longitudinal crevasse zones. The surface undulations are similar in form to those on Slessor Glacier in area 4 B (see Fig. 5) but possibly of greater amplitude.

This topography is gradational with that of area 2 B where a reticular pattern of 4-km wavelength features fades towards both area 2 C and the Shackleton Range. At the boundary with Filchner Ice Shelf the 'ice wall' (Blaiklock and others, 1966 p. 15) encountered by TAE forms a prominent 1–2-km-wide feature in Landsat imagery and probably accounts for about half of the mapped rise of 300 m over 8 km.

Apart from the longitudinal furrows area 2 C lacks short wavelength undulations. VHRR imagery shows faint 25 km wavelength features south of the eastern Shackleton Range and two prominent 10-km wavelength north–south trending features north of the eastern most outcrops of area 1 B.

Shackleton Range (areas 3 A, 3 B, and 3 C)

The Shackleton Range is composed mainly of metamorphic rocks (Clarkson, 1972). Its physiography has been described by Stephenson (1966) and Skidmore and Clarkson (1972). Remnants of an undulating peneplain are preserved as summit plateaux on the highest peaks (mainly in the south), rising from *c.* 1300 m in the west to *c.* 1600 m in the east. Local variations in level of up to 200 m are probably due in part to faulting. The various mountain ridge and valley systems have periods mainly in the range 4–8 km and on this scale bedrock relief is probably only a little greater than the maximum of *c.* 700 m exposed; a few valleys are ice free.

Features along the margins of the range described by Skidmore and Clarkson (1972) are seen clearly by Landsat. Peaks along the north–south trending western margin rise 500–600 m above the ice of area 2 B. In the east the range gradually disappears under the ice sheet at *c.* 1600 m but frequent 1-km wavelength ice features, and probably a rock outcrop at 79° 45′ S, 17° 10′ W, mark its continuation beneath the ice. Between 30° and 22° W the southern margin of the range as shown in Fig. 4 is the locus of the southernmost rock outcrops and kilometre-scale ice features but the major crevasse zones of Recovery Glacier lie over 10 km to the south. The southern margin of the easternmost part of the range consists of a 'series of crevassed terraces' (Fuchs and Hillary, 1958, p. 108), which are seen in VHRR imagery to extend for some 150 km eastwards from the inflexion in the margin at 22° W. Along the northern margin of the range, west of 25° W, 1–2-km wavelength ice features extending beyond most of the outcrop cease abruptly at the margin of the heavily crevassed Slessor Glacier. Eastwards to 21° W there is a broader gradational zone (area 3 B) between the northern outcrops and the crevasses of the glacier. The northern boundary of the inferred sub-ice extension of the range to the east is marked by the disappearance of 8 km wavelength features in Slessor Glacier. Overland traverses from Halley Bay (Noble, 1968) turned westward towards the Shackleton Range at this change in topography but no major change in the level of the ice was reported.

Slessor Glacier (*areas 4A, 4B, 4C, and 4D*)

Zones of intense crevassing characterizing the lower part of Slessor Glacier are continuous with flow lines on the Filchner Ice Shelf (Crabtree and Doake, 1980). The margin of the ice shelf is indistinct but probably lies close to the western limit of 3–5-km wavelength ice features in the north-western part of area 4A (see Fig. 5). Except for the crevasse zones the remainder of area 4A has only very faint long wavelength (*c.* 20 km) features. The final 50 km of the glacier merges with Bailey Ice Stream but for 120 km east of Parry Point the northern margin is an ice scarp 100–200 m high in the west but progressively lower towards the east.

The trend of this scarp is continued across the glacier by a slightly broader feature which produces a swing in the trend of the longitudinal crevasse zones and forms a limit to the 3–8-km wavelength features characteristic of area 4B. The undulating topography and the bifurcating form of this upper part of the glacier was first described by Fuchs (in Fuchs and Hillary, 1958, p. 108). Although much less crevassed than the lower reaches, the circuitous route of overland parties from Halley (Fig. 2) defines the limit of an area of difficult terrain. The most severe crevassing encountered on these journeys (Samuel, 1968*a*, *b*; Noble, 1968) was part of the zone extending along and westwards from the northern side of area 4D. The same crevasse zone some 75 km to the north-east forced the termination of an eastward tractor traverse (Hoy, 1970) after 8-km-wavelength features with heights (crest–trough) of *c.* 23 m (Peel, 1976, fig. 1b) had been crossed; barometer observations made on the southward traverse suggest undulations of up to twice this height.

The longitudinal crevasse zones indicate that most of the flow of the glacier passes around a small area of featureless ice (4C) and to the north-west of area 4D, which is mainly featureless but locally has groups of short wavelength (1–2 km) features. To the south area 4D has a more gradational margin with the southern branch of Slessor Glacier.

Theron Mountains (*areas 5A and 5B*)

The Theron Mountains are composed of horizontally bedded sedimentary rocks intruded by dolerite sills up to 200 m thick (Stephenson, 1966; Brook, 1972*b*). The physiography has been described by Stephenson (1966), Wornham (1969) and Brook (1972*a*). The main outcrops are part of a 100-km-long, north-west facing rock and ice escarpment with a maximum exposed relief of *c.* 900 m at Mount Faraway (2140 m). Westwards from Mount Faraway the top of the escarpment descends to *c.* 250 m at Parry Point but to the east it maintains a level of *c.* 1000 m. At its foot the Bailey Ice Stream descends from *c.* 800 m at 26° W to *c.* 220 m at Mount Faraway (A. Johnston, unpublished map).

The outcrops have a characteristic 'cliff and ledge' topography, with steep rock scarps capped by vertically jointed sills. A similar pattern of ice scarps (*c.* 100 m high) and ledges south of the rock escarpment is well displayed by Landsat (Fig. 5) and grades into a large area (5B) with short (1 km) wavelength features. At its southern margin this area gives way abruptly to more subdued topography (area 5A) with widely distributed, faint, 2-km wavelength features. Visual and barometric observations made during the reconnaissance circuit of area 5A (Samuel, 1968*a*, *b*) indicate that it has an almost uniform slope of 0.6° to the south. The boundary with Slessor Glacier in area 4B is subparallel to the longitudinal crevasse zones but there appears to be little change in ice level.

Bailey Ice Stream (area 6)

The Bailey Ice Stream was referred to as 'Main Glacier' by Brook (1972*a*) who estimated its width to be approximately 50 km. Only the southern margin against the Theron Mountains is well-defined but a series of 1–2-km wavelength ice features 55 km to the north-west shown by Landsat, probably the ice escarpment mentioned by Brook (1972*a*, p. 25), may mark the north-western margin. Both the altitude data (Fig. 2) and the trend of longitudinal crevasse zones in the upper part of Slessor Glacier suggest that the ice stream receives little ice from east of 10° W. The boundary with Filchner Ice Shelf is less distinct than that of the Slessor Glacier.

The largest ice surface features in the ice stream and the basin feeding it are a group of spur-like north-west trending ridges, of wavelength 10 km and height *c.* 50 m (A. Johnston, unpublished map), some 15 km north-west of the Theron Mountains (see Fig. 5). In the remainder of area 6, faint 2–5-km wavelength features are present locally but, apart from two north-west trending features and four areas with abundant 4-km wavelength undulations, no clear pattern is apparent. The altitude profile of Peel (1976) shows 3-km wavelength features of height 15 m at the edge of one of t undulating areas but elsewhere in area 6 it is featureless.

The ice sheet adjacent to the coast (areas 7–11)

West of *c.* 33° W (area 7A) most of the features seen in the imagery have wavelengths of *c.* 2 km. A series of 1–2 km wavelength features forms an outward facing scarp which almost completely encloses the highest ground. In the north-west it is incised by narrow (2–5 km wide) glaciers and locally merges with lower scarps extending inland from the coast. To the east of the north–south trending section of the scarp at 33° W is a 15-km-wide belt of ice with no visible features.

The small outcrops of igneous rocks in this area (Augenbaugh and others, 1965; Marsh and Thomson, 1984) all occur where the upper and lower scarps are close together; Moltke Nunataks are rock windows in the face of an ice cliff representing both features, whereas Littlewood Nunataks (283 m) and Bertrab Nunatak appear to be breaches in the top of the lower scarps.

Between 21° and 33° W the ice slopes descending towards the Weddell Sea have abundant 1.5–2.5-km wavelength undulations. Those within area 8 have a lower amplitude and smaller average wavelength than those in area 7B, which extends almost to the crest of the major ice ridge. As this crest is approached, the features become more subdued and widely spaced and there is a gradation into the almo featureless terrain of area 6. The altitude profiles of Bailey and Evans (1968) and Pee (1976) show that the undulations in area 7B typically have two or three times the amplitude of those in area 8; more widely spaced undulations in area 7C are also seen. The radio-echo ice sounding profile of Bailey and Evans (1968) shows that the change in surface morphology corresponds to a rapid change in mean bedrock level from *c.* 100 m below sea level (with a relief of *c.* 200 m over 2 km) in area 8 to *c.* 300 m a.s.l (and relief of *c.* 400 m over 2 km) in area 7B (see Figs. 2 and 3).

The morphology of the ice surface inland of Brunt Ice Shelf has been described by Ardus (1965). Icefalls, seen as 1-km wavelength features in the imagery, are abundant up to altitudes of 400–600 m and slopes locally reach 5°. The major feature of this area is the Stancomb–Wills Ice Stream. Landsat shows associated longitudinal features converging towards a 20-km-wide zone at its entry to the ice shelf. The short wavelength features of area 8 are replaced in area 9A by larger (4-km wavelength) features which cease at the margin with the ice shelf. The longitudinal features

originate in a large area (9C) characterized by many prominent 1-km wavelength features, which have the appearance of a series of north-westward facing scarps. These are the most prominent features seen remote from rock outcrops in the region. The same topography is visible in VHRR imagery and gives way south-eastwards to almost featureless higher ground.

Stancomb–Wills Ice Stream and the glacier Veststraumen (area 11) are separated by a 100-km-wide, north–west trending ridge (area 10). Landsat shows 1–2-km wavelength features to be abundant in the lower 500 m, less so towards the crest. On the north-east side, outcrops of high grade gneiss forming Mannefallknausane rise to *c.* 1230 m (Blundell and Winterton, 1962; Ardus, 1965; Juckes, 1968). The ice descends between them in a series of crevassed slopes and icefalls seen in the imagery as features with wavelength 1 km and less. Similar features are typical of several areas on the flanks of the ridge on the south side of Vestraumen and are often aligned parallel to the glacier margin.

The surface of Veststraumen is characterized by irregular, mainly transverse, 5-km wavelength undulations. Its topography is similar to that of the upper Slessor Glacier (area 4B) but longitudinal features are not seen. There is a reduction in the undulation wavelengths (to *c.* 3 km) as the glacier approaches the ice shelf and the abrupt disappearance of these features is assumed to mark the ice shelf boundary. The north-eastern margin of the glacier is indistinct but a change to mainly shorter-wavelength undulations occurs along a line parallel to and 65 km north-east of the south-western margin. Blundell and Winterton (1962) mentioned no increase in the intensity of crevassing at their crossing (Fig. 2) of the south-western and north-eastern margins.

Heimefrontfjella (area 12)

Heimefrontfjella is a dissected, north–east trending escarpment composed mainly of gneiss (Juckes, 1972). Its physiography has been discussed by Swithinbank (1959), Ardus (1964), Worsfold (1967) and Juckes (1972). In the north-east, undulating summit plateaux at *c.* 2100 m bear small areas of gently dipping sedimentary rocks and terraced outcrops of basaltic lavas, but in the south-west, the gneiss outcrops rise to 2900 m and summit plateaux are not seen. The lowest outcrop is at *c.* 1200 m and the maximum exposed relief is *c.* 800 m.

The ice sheet to the south-east has a low slope and Landsat shows widely distributed 1–2-km wavelength undulations for over 60 km inland of the outcrops. A steeper slope descending to the north-west has features of similar wavelength, which disappear along an indistinct line parallel to the range before the longer wavelength features of Veststraumen become conspicuous. Faint longitudinal features support the conclusion of Worsfold (1967) that the drainage from inland is largely around, rather than through the range. Ice flowing around the south-western end towards the Stancomb–Wills Ice Stream forms an indistinct boundary between the range and area 9C.

Relationship of Surface Features to Bedrock Topography

Observations and photographs from aircraft allowed Swithinbank (1959) to infer that ice surface undulations in Dronning Maud Land were mainly related to bottom topography and that the steeper and more varied slopes correspond to areas of thinner ice. Seismic soundings in the same area (Robin, 1958) showed that steps in the downslope profile overlie subglacial ridges. An analysis of the relationship between measured ice surface and bedrock profiles was given by Budd and Carter (1971). At

right angles to the flow, bedrock and surface profiles are approximately in phase, but in the direction of flow, the surface profile lags behind that of the bedrock by about one quarter of the wavelength, such that the steepest slopes correspond to bedrock elevations.

Budd and Carter (1971) found that surface profiles in the direction of ice flow were dominated by wavelengths about three or four times the ice thickness. They presented a model of ice flow that predicts that the damping of the bedrock topography by the ice is at a minimum for wavelengths of 3.3 ice thicknesses; shorter wavelengths are damped out rapidly, longer wavelengths less so. Hence, for a uniform distribution of amplitudes in the bedrock spectrum, these wavelengths would be expected to dominate the surface profile. The damping factor (bedrock amplitude/surface amplitude) at this minimum varies the the square of the ice thickness and inversely with the velocity and viscosity. Budd and Carter give values of between 10 and 25 for the Wilkes ice sheet (eastern Antarctica) and between 5 and 30 for the much larger Greenland ice sheet. In both of these cases a roughly inverse relationship between velocity and viscosity results in the damping varying mainly with the ice thickness.

More recent theories of ice flow (Hutter and others, 1981; Whillans and Johnsen, 1983) account less readily for the observed dominance of wavelengths of three to four ice thicknesses, although greater damping for shorter wavelengths is a feature of all models. Hutter and others (1981) found that dominant wavelengths of between three and five ice thicknesses could occur only if the sliding mechanism and inclination were appropriate. Whillans and Johnsen (1983) modelled conditions under which transfer of undulations to the surface shows a peak, but not a maximum at these wavelengths, and they suggest that a lower abundance of longer wavelengths in the bedform contributes to the observed maximum at the surface.

Thus, the features seen in the imagery are a variably damped, filtered and phase-shifted response to the bedrock topography. The surface undulations a few metres or tens of metres high seen in the imagery are probably produced by bedrock features about an order of magnitude higher. Areas with relatively uniform patterns of surface undulations probably have similarly uniform depths to bedrock. Although individual features reflect corresponding bedrock features, and where linear their trends should remain within a few degrees of the bedrock trends, they will probably not be azimuthally or spectrally representative.

Little can be inferred from gradational changes in surface topography but discontinuities reflect changes in the flow or thickness of ice or in the bedrock topography and hence will, in general, signal a discontinuity in the bedrock morphology. In general, an increase in the dominant wavelength of undulations and/or a reduction in their amplitude will indicate an increase in the ice thickness, but this could be distorted by radical changes in the bedrock spectrum or ice flow. The largest variations in ice flow are associated with ice streams and major glaciers such as the Slessor and Recovery. In addition to large velocity changes at their margins it can be expected that, at some point in their descent, pressure melting will allow basal sliding whilst the surrounding ice remains frozen to its bed (Rose, 1979), a change in boundary conditions likely to be associated with increased erosion of the bed (Hutter and Olunluyu, 1981) and an increase in the damping. However, it can be assumed that, as has been shown in Marie Byrd Land (Rose, 1979), the ice streams are situated over bedrock channels, and an increase in ice thickness can be inferred from the characteristic change to longer wavelength undulations across their margins.

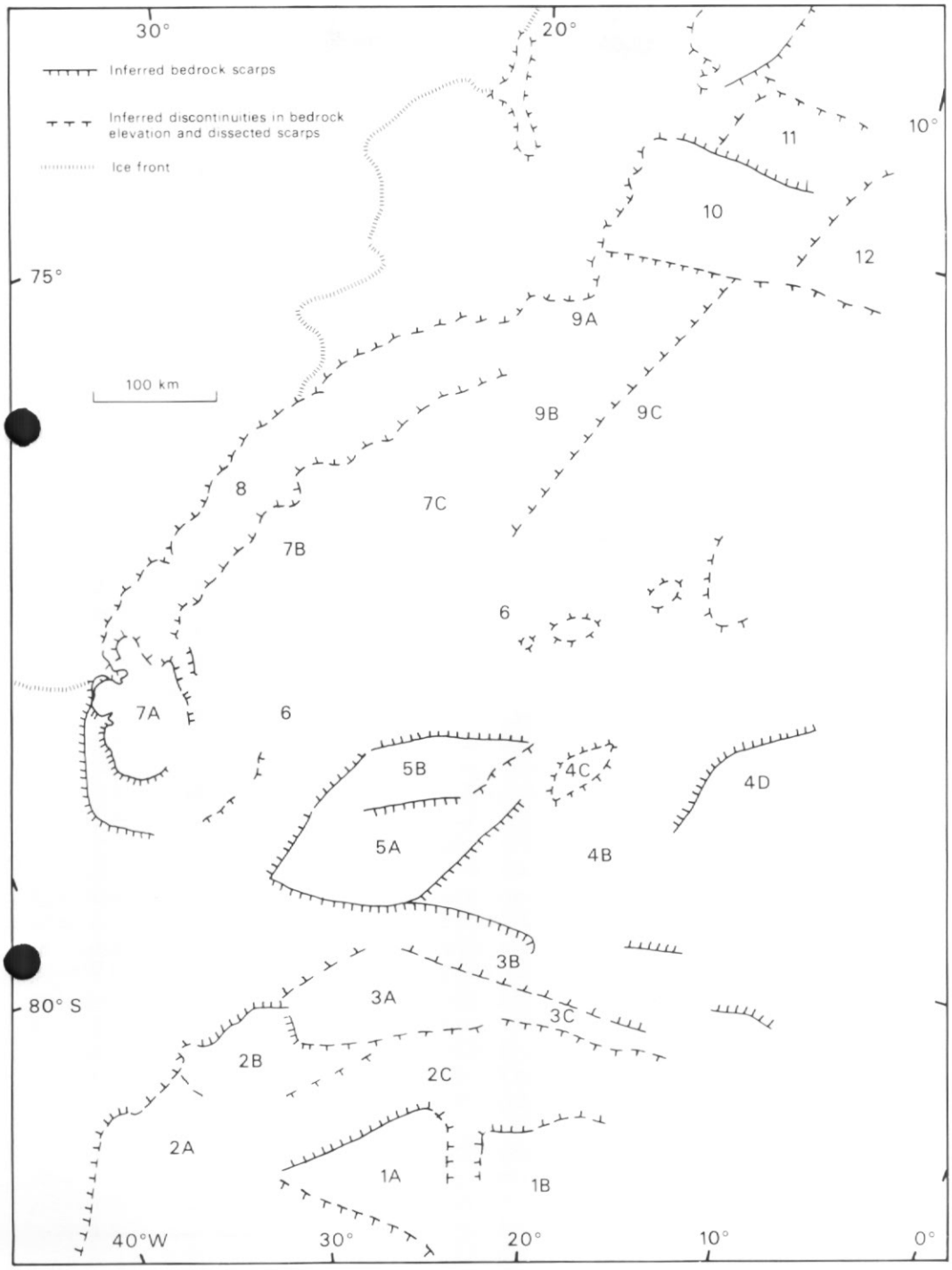

Fig. 7. Inferred bedrock features in Coats Land and Dronning Maud Land. Boundaries of Physiographic zones are shown more fully in Fig. 4.

Inferred bedrock features in Coats Land

Subglacial scarps and other changes in bedrock elevation inferred from the imagery are shown in Fig. 7. In making this interpretation abrupt increases in the dominant wavelength of undulations were assumed to correspond to increases in ice thickness. This change is nowhere seen to occur at an increase in the ice surface elevation, leading to the further inference that it is most likely to be due to a markedly lower bedrock elevation in the area with the larger wavelength features. At almost all of the changes in topography recognized, there is known to be a decrease in surface elevation as the longer-wavelength terrain is entered, an observation that tends to discount the alternative interpretation that the surface changes are due mainly to changes in the bedrock spectrum. The only bedrock feature mapped solely on the basis of a change in the amplitude of surface features is that along the boundary between areas 8 and 7B.

Discussion

Many of the inferred bedrock features are approximately linear and trends close to those prominent in the Theron Mountains area recur throughout the region; several of these lineaments are nearly collinear. Their prominence at the margins of the main outcrop areas suggest that the region is a mosaic of segments bounded by faults with these trends. The lack of dissection on many of the inferred scarps may imply youth and one of the few earthquakes recorded in Antarctica occurred below Slessor Glacier (Kaminuma and Ishida, 1971). Masolov and others (1980) suggested that the presence of the ice sheet has prevented the deposition of clastic sediments which obscure graben morphology elsewhere in the world. Subaerial erosion processes must have acted prior to its development but the more uniform erosion by the ice sheet is probably more responsive to major bedrock changes, which are made more conspicuous at the ice surface by the filtering out of much small-scale topography. The continuity of features near areas known to contain sub-horizontal sedimentary strata contrasts with the dissected margins of the basement areas. These conspicuous lineaments may be scarps produced by joint-controlled erosion of bedding units or sills, as seen in the Theron Mountains, rather than the exact loci of major faults. However, many are probably below sea level, which could also account for their lack of dissection.

The large scale of individual features and the apparent consistency of orientation throughout the area suggests that they are related to regional structures. The northern and western margins of the continental area described here appear to have originated during Mesozoic rifting (Masolov and others, 1980; Hinz, 1981; Hofmann and Weber, 1983). Lineaments sub-parallel to the escarpment and to the major valleys of the Theron Mountains may indicate the presence of fractures associated with rifting along the 'Weddell Sea' and 'Filchner Ice Shelf' margins of the continent respectively. The east–west trending features along the south of area 5B and the Shackleton Range are parallel to the foliation in the latter (Clarkson, 1982) and may thus be an older 'basement' trend.

Proper assessment of the significance of the ice surface features in terms of the subglacial geology and regional structure will require a detailed comparison with known outcrop geology and fracture patterns. The main conclusion to be drawn from this account of the area is that in addition to providing geographic detail in poorly surveyed areas of the ice sheet, the satellite images reveal major lineaments which fill blanks on the map and indicate some major structural trends with which to view geological and geophysical interpretations of the area. The interpretation of the ice

surface could be tested by airborne radio-echo sounding, and if validated would suggest that satellite imagery could assist greatly during the interpolation between widely spaced flight lines.

ACKNOWLEDGEMENTS

I wish to thank Drs C. W. M. Swithinbank, D. A. Peel and N. W. Riley for the loan of Landsat images, barometric profiles and manuscripts maps respectively, and Dr P. D. Clarkson for guidance when seeking out reports of overland journeys from Halley Bay. Drs C. W. M. Swithinbank and P. D. Clarkson made valuable comments on the manuscript.

Received 12 February 1985; accepted in revised form 25 April 1985

REFERENCES

ARDUS, D. A. 1964. Some observations at the Tottanfjella, Dronning Maud Land. *British Antarctic Survey Bulletin*, No. 3, 17–20.

ARDUS, D. A. 1965. Morphology and regime of the Brunt ice shelf and adjacent inland ice, 1960–61. *British Antarctic Survey Bulletin*, No. 5, 13–42.

AUGHENBAUGH, N. E., LOUNSBURY, R. W. *and* BEHRENDT, J. C. 1965. The Littlewood Nunataks, Antarctica. *Journal of Geology*, **73**, 889–94.

BAILEY, J. T. *and* EVANS, S. 1968. Radio echo-sounding on the Brunt Ice Shelf and in Coats Land, 1965. *British Antarctic Survey Bulletin*, No. 17, 1–12.

BLAIKLOCK, K. V., STRATTON, D. G. *and* MILLER, J. H. 1966. Survey. *Transantarctic Expedition 1955–58 Scientific Reports*, No. 15, 27 pp.

BLUNDELL, G. *and* WINTERTON, M. J. 1962. Report of Sledging journey to the north and east of the Dalgleish ice falls. 24 Oct–24 Dec, 1961. British Antarctic Survey travel report AD6/2Z/K2/1962, 16 pp. [Unpublished.]

BROOK, D. 1972*a*. Physiology and glacial morphology of the Theron Mountains, *British Antarctic Survey Bulletin*, No. 27, 25–38.

BROOK, D. 1972*b*. Stratigraphy of the Theron Mountains. *British Antarctic Survey Bulletin*, No. 29, 67–90.

BUDD, W. F. *and* CARTER, D. B. 1971. An analysis of the relation between the surface and bedrock profiles of ice caps. *Journal of Glaciology*, **10**, 197–209.

CLARKSON, P. D. 1972. Geology of the Shackleton Range: a preliminary report. *British Antarctic Survey Bulletin*, No. 31, 1–15.

CLARKSON, P. D. 1982. Tectonic significance of the Shackleton Range. (*In* CRADDOCK, C. *ed. Antarctic geoscience*. Madison, University of Wisconsin Press, 835–9.)

COSLETT, P. H., GUYATT, H. M. *and* THOMAS, R. H. 1975. Optical levelling across an Antarctic ice shelf. *British Antarctic Survey Bulletin*, No. 40, 55–63.

CRABTREE, R. D. *and* DOAKE, C. S. M. 1980. Flow lines on Antarctic ice shelves. *Polar Record*, **20**, 31–7.

DREWRY, D. J. 1983. The surface of the Antarctic Ice Sheet. (*In* DREWRY, D. J. *ed. Antarctica: glaciological and geophysical folio*. Scott Polar Research Institute, Cambridge University, Sheet 2.)

DREWRY, D. J. *and* JORDAN, S. R. 1983. The bedrock surface of Antarctica. (In DREWRY, D. J. *ed. Antarctica: glaciological and geophysical folio*. Scott Polar Research Institute, Cambridge University, Sheet 3.)

FUCHS, V. E. *and* HILLARY, E. 1958. *The crossing of Antarctica*. London, Cassell, 338 pp.

GRIKUROV, G. E. (*ed.*) 1978. Tectonic Map of Antarctica at 1:10,000,000. Leningrad, Research Institute of the Geology of the Arctic.

HINZ, K. 1981. A hypothesis on terrestrial catastrophies. Wedges of very thick oceanward dipping layers beneath passive continental margins. Their origin and palaeo-environmental significance. *Geologisches Jahrbuch E22*, 3–28.

HOFMANN, J. *and* WEBER, W. 1983. A Gondwana reconstruction between Antarctica and Africa. (*In* OLIVER, R. L., JAMES, P. R. *and* JAGO, J. B., *eds. Antarctic earth science*. Canberra, Australian Academy of Science, and Cambridge, Cambridge University Press, 584–9.)

HOY, D. J. 1970. Glaciological traverse, Summer 1970. British Antarctic Survey travel report AD6/2Z/K6/1970. [Unpublished.]

HUTTER, K., LEGERER, F. *and* SPRINK, U. 1981. First order stresses and deformations in glaciers and ice sheets. *Journal of Glaciology*, **27**, 227–270.

HUTTER, K. *and* OLUNUYU, V. U. S. 1981. Basal stress concentrations due to abrupt changes in boundary conditions: cause for high till concentrations at the bottom of a glacier. *Annals of Glaciology*, **2**, 29–33.

JUCKES, L. M. 1968. The geology of Mannefallknausane and part of Vestfjella, Dronning Maud Land. *British Antarctic Survey Bulletin*, No. 18, 65–78.

JUCKES, L. M. 1972. The geology of north-eastern Heimefrontfjella, Dronning Maud Land. *British Antarctic Survey Scientific Reports*, No. 65, 43 pp.

KAMINUMA, K. *and* ISHIDA, M. 1971. Earthquake activity in Antarctica. *Antarctic Record*, No. 42, 55–60.

LEVANON, N. *and* BENTLEY, C. R. B. 1979. Ice elevation map of Queen Maud Land, Antarctica, from balloon altimetry. *Nature*, **278**, 842–44.

MARSH, P. D. *and* THOMSON, J. W. 1984. Location and geology of nunataks in north-western Coats Land. *British Antarctic Survey Bulletin*, No. 65, 33–39.

MARTIN, P. J. *and* SANDERSON, T. J. O. 1980. Morphology and dynamics of ice rises. *Journal of Glaciology*, **25**, 33–45.

MASOLOV, V. N., KURANIN, R. G. *and* GRIKUROV, G. E. 1980. Crustal structures and tectonic significance of Antarctic rift zones (from geophysical evidence). (*In* CRESSWELL, M. M. *and* VELLA, P. *eds. Gondwana five*. Rotterdam, A. A. Balkema, 303–10.)

NOBLE, P. H. 1968. Halley Bay to Shackleton Range outward traverse, Spring 1968. British Antarctic Survey travel report AD6/2Z/K7/1968. [Unpublished.]

PEEL, D. A. 1976. Snow accumulation, conductance and temperature inland from Halley Bay. *British Antarctic Survey Bulletin*, No. 43, 1–13.

PRATT, J. G. D. 1960. Seismic sounding across Antarctica. *Transantarctic Expedition 1955–58 Scientific Reports*, No. 3, 69 pp.

ROBIN, G. DE Q. 1958. Seismic shooting and related investigations. *Scientific Results. Norwegian–British–Swedish Antarctic Expedition, 1949–52*, **5**, 134 pp.

ROSE, K. 1979. Characteristics of ice flow in Marie Byrd Land, Antarctica. *Journal of Glaciology*, **24**, 63–75.

SAMUEL, M. M., 1968*a*. Route reconnaissance around the Slessor Glacier, B.A.T., 9 Nov.–29 Nov. 1967. British Antarctic Survey travel report AD6/2Z/K19/1967. [Unpublished.]

SAMUEL, M. M. 1968*b*. Summer muskeg journey towards the Shackleton Range, via the Theron Mountains. British Antarctic Survey travel report AD6/2Z/K20/1967. [Unpublished.]

SKIDMORE, M. J. *and* CLARKSON, P. D. 1972. Physiography and glacial geomorphology of the Shackleton Range. *British Antarctic Survey Bulletin*, No. 30, 69–80.

STEPHENSON, P. J. 1966. Geology. 1. Theron Mountains, Shackleton Range and Whichaway Nunataks (with a section on palaeomagnetism of the dolerite intrusion by D. J. Blundell). *Transantarctic Expedition Scientific Reports*, No. 8, 79 pp.

STURGEON, L. J. S. *and* RENNER, R. G. B. 1983. New Doppler satellite controlled gravity stations in Antarctica. *British Antarctic Survey Bulletin*, No. 59, 9–14.

SWITHINBANK, C. W. M. 1959. The morphology of the inland ice sheet and nunatak areas of western Dronning Maud Land. *Scientific Results. Norwegian-British-Swedish Antarctic Expedition 1949–52*, **3D**, 97–117.

SWITHINBANK, C. W. M. 1977. Glaciological research in the Antarctic Peninsula. *Philosophical Transactions of the Royal Society*, **279**, 161–83.

SWITHINBANK, C. W. M. *and* LANE, C. 1977. Antarctic mapping from satellite imagery. (*In* PEEL, R. F., CURTIS, L. F. *and* BARRETT, E. C. Remote sensing of the Terrestrial Environment. London, Butterworth, 212–21.)

THORARINSSON, S., SAEMUNDSSON, K. *and* WILLIAMS, R. S. 1973. ERTS-1 image of Vatnajökull: analysis of glaciological, structural and volcanic features. *Jökull*, No. 23, 7–17.

WARREN, S. G. 1982. Optical properties of snow. *Reviews of Geophysics and Space Physics*, **20**, 67–89.

WHILLANS, I. M. *and* JOHNSEN, S. J. 1983. Longitudinal variations in glacial flow: theory and test using data from the Byrd Station strain network, Antarctica. *Journal of Glaciology*, **29**, 78–97.

WORNHAM, C. M. 1969. Ice-movement measurements in the Theron Mountains. *British Antarctic Survey Bulletin*, No. 21, 45–50.

WORSFOLD, R. J. 1967. Physiography and glacial geomorphology of Heimefrontfjella, Dronning Maud Land. *British Antarctic Survey Bulletin*, No. 11, 49–57.